Polymer 41 (2000) 7289–7293

Polymer Communication

Solid-state fast magic angle spinning ^{19}F NMR studies of morphology in poly(vinylidene fluoride)

Tsao-Wen Su[a], Der-Lii M. Tzou[b,*]

[a]*Physical Chemistry Section, Chemical Systems Research Division, Chung-Shan Institute of Science and Technology, Tao-Yuan, 325, Taiwan, ROC*
[b]*Institute of Chemistry, Academia Sinica, Nankang, Taipei 115, Taiwan, ROC*

Received 2 June 1999; received in revised form 13 September 1999; accepted 26 November 1999

Abstract

Solid-state ^{19}F NMR in combination with fast magic angle spinning at a speed of 35 kHz has been applied to examine the morphology of poly(vinylindene fluoride) samples by effectively suppressing dipolar interactions of the same order. A Lorentzian lineshape fitting analysis applied to the fast magic angle spinning spectrum was able to determine accurately the relative contents for the various domains: crystalline phase, 41%; amorphous regions, 54%; defect segments, 5%; with ±3% error limits. Chemical shift anisotropies were also retrieved from sideband intensities: the amorphous component showed rather small anisotropy compared to that of the crystalline domain. Phase separation, in terms of the crystalline and non-crystalline domains, was distinguished by 2D spin exchange experiments, where cross-peaks were found not to be caused by chain conformation reorientations, but instead by spin diffusion. Evidence of the spin diffusion behavior mediated by unsuppressed homonuclear dipolar interactions has allowed us to examine molecular proximity under fast MAS conditions. © 2000 Elsevier Science Ltd. All rights reserved.

Keywords: Poly(vinylidene fluoride); Fast magic angle spinning; Chemical shift anisotropy

1. Introduction

Poly(vinylidene fluoride) (PVDF) has attracted much scientific and industrial attention over the years because of its excellent processability, superior mechanical characteristics, pyro-electricity properties, and extremely high fluidity in a wide range of working temperatures. Transformations among the different crystalline forms are possible by stretching, high-pressure, annealing or poling (for review articles see Ref. [1]). Crystalline phases incorporating various chain conformations have been studied by X-ray crystallography [2–4]. For example, the α-crystalline state has been found to exhibit an alternative chain conformation with a TGT$\bar{\mathrm{G}}$ pattern, and the β-crystalline phase shows all-*trans* chain conformation. Investigations of phase transformation require detailed characterization of the overall chain morphology. Unfortunately, until now, such quantitative analysis has been limited.

It is well known that the solid-state NMR is a very valuable technique for the characterization of polymer morphology [5]. In particular, solid-state magic angle-spinning (MAS) ^{19}F NMR has proven to be extremely powerful in studying polymers containing ^{19}F. There are several advantages of exploiting the ^{19}F nucleus. One is its high gyromagnetic ratio and natural abundance leading to high sensitivity. Secondly, the ^{19}F NMR spectrum provides a broad dispersion in chemical shifts that facilitates resonance assignments by correlating the signals with sample morphology. Tonelli et al. [6] reported the chemical shift assignments of PVDF in the high-resolution liquid-state ^{19}F spectrum. These workers identified peaks associated with head-to-tail (H–T) and head-to-head:tail-to-tail (H–H:T–T) defect segments, and interpreted these results in terms of bond-rotation probabilities and γ *gauche* effects. Ferguson and Brame [7] have calculated ^{19}F chemical shifts and Bernoullian distribution probabilities related to H–T in the PVDF solution phase. In the solid-state, however, the detrimental line-broadening effect remains a prohibitive issue. The broadening effect can be heterogeneous, originating from distributions of isotropic chemical shifts caused by the dispersion in molecular packings, or homogeneous broadening, arising from residual homo- ^{19}F–^{19}F and/or hetero-nuclear ^{19}F–^{1}H dipolar interactions. The former is linearly field-dependent, but MAS speed independent for sufficiently small dispersions and the latter can be averaged by rapid molecular motions as well as sample rotation. For

---

* Corresponding author. Tel.: +886-2-2789-8524; fax: +886-2-2783-1237.

E-mail address: tzou@ccvax.sinica.edu.tw (D.-L.M. Tzou).

0032-3861/00/$ - see front matter
PII: S0032-3861(99)00884-8

quantitative analysis, it has to be ensured that the former is retained and the latter is minimized. Experimentally, one might consider implementing a multiple RF pulse sequence such as CRAMPS [8,9] to suppress the first-order dipolar Hamiltonian, and allow only the chemical shift to evolve. Unfortunately, despite hardware developments and tedious/meticulous calibrations, this experiment fails with samples that have large chemical shift dispersions. This is the situation with PVDF.

As an alternate, Holstein et al. [10] have used the ^1H–^{19}F cross-polarization (CP)/MAS method to characterize polymorphism by increasing the MAS speed up to 17 kHz on a 4 mm rotor. However, even this speed is too low to effectively suppress the dipolar broadening, where a ^{19}F homonuclear dipolar strength nearly 30 kHz is estimated based on the internuclear ^{19}F–^{19}F distance of 1.568 Å [11]. It is demonstrated that the unsuppressed dipolar line broadening not only smears out the spectrum, but also introduces an inaccuracy in analysis of relative domain contents where spectral fitting is employed.

An effective way to remove the dipolar broadening, of course, is to increase the MAS speed. Here, we report the successful application of the fast MAS technique to the PVDF problem, MAS speeds up to 35 kHz are demonstrated. This speed was fast enough to effectively suppress the residual dipolar broadening effect in PVDF. Additionally, we have employed 2D (two-dimensional) fast MAS spectroscopy to provide information about sample morphology and molecular proximity.

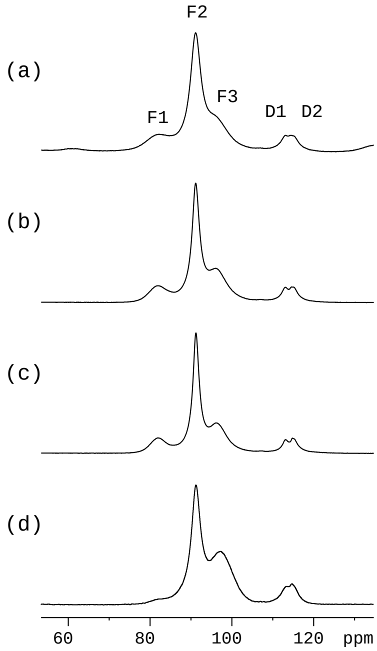

Fig. 1. Solid-state ^{19}F NMR spectra acquired by fast MAS at: (a) 20 kHz; (b) 30 kHz; and (c) 35 kHz, respectively; (d) is same as (c), except that sample treated by annealing process described in experimental section. All spectra were acquired at room temperature and were referenced to $CFCl_3$ at 0 ppm.

2. Experimental

Two PVDF samples were investigated in the present solid-state NMR study. The first sample consists of powdered PVDF ($M_n = 190,000$, $M_w = 519,000$), a commercial product KYLAR 500 from Ausimont Co. Second, the annealed sample was carried out as follows; the PVDF powder was dissolved in *N*-Methyl-2-pyrrolidone, (C_5H_9NO, NMP), and the well-mixed gel was kept in the oven for 24 h at 160°C near the PVDF melting temperature as the solvent gradually evaporated. At the end the sample was gradually cooled down to room temperature within three hours and ready for the NMR measurements.

The fast MAS experiment was performed on the Bruker DMX 500 spectrometer operating at a ^{19}F Larmor frequency of 467.13 MHz. An upper limit speed of 35 kHz was reached within 1 Hz variation controlled by automated pneumatic unit. Only, a single pulse ($\pi/2$) was used. A total of 1k data was acquired using a 90° pulse length of 1.6 μs and spectral window of 50 kHz, with zero-filling to 4k. In chemical shift anisotropy measurements, at MAS speed of 35 kHz, one-dimensional (1D) experiment was performed at an extra-high field spectrometer operating at ^{19}F Larmor frequency of 752.8 MHz in order to increase the spectral dispersion, and therefore, more spinning sidebands, for greater accuracy.

Spin–lattice relaxation time T_1 measurements were done by the inversion recovery sequence $180_x° - \tau - 90_y°$, where τ varied from 10 μs to 3 s. Spin–spin relaxation time T_2 was determined by $90_x° - \tau - 180_y°$ sequence, with τ sampling in the range of 170 μs–1 ms. The experiments were performed at MAS speed of 35 kHz.

The 2D exchange [12,13] data were acquired with 200 t_1 increments of 10 μs for studying spin exchange behavior. A total of 1 k data points were collected with 1024 scans, 4.5 μs excitation pulse, spectral window of 40 kHz, 5.0 s repetition rate and with further zero-filling to 4K. Experiments were also performed in the presence of 180° pulse trains for spin diffusion enhancement [14,15]; and the pulse sequence is given in Fig. 2. All spectra were collected at ambient room temperature and were referenced to $CFCl_3$ at 0 ppm.

3. Results and discussion

3.1. Fast MAS ^{19}F spectrum

Fig. 1a–c shows a set of the 1D solid-state ^{19}F MAS PVDF spectrum, with the sample spinning at 20, 30 and 35 kHz, respectively. Holstein et al. [10] have reported that the PVDF spectrum exhibits five isotropic resonances attributed to amorphous domains (at −91.2 ppm), crystalline domains (−81.8 and −96.1 ppm), and defect structures (−113.1 and −115.0 ppm) arising from head-to-head

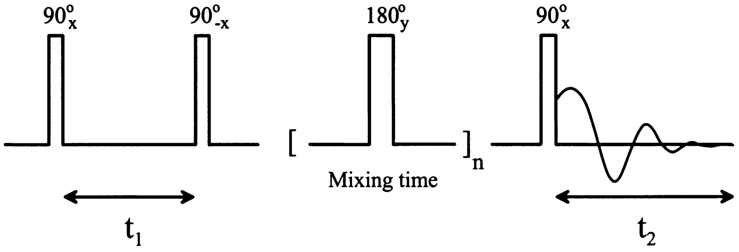

Fig. 2. Two-dimensional exchange pulse sequence with additional 180° pulse trains applied during mixing period.

(H–H) and tail-to-tail (T–T) irregular addition of monomers. For sake of discussion here, these components are denoted as F2, F1, F3, D1 and D2, respectively, see Fig. 1a. Presumably the individual intensity and its lineshape can be used to infer local chain environments and sample morphology, provided that one can perform lineshape-fitting analysis analogous to curve integration applied to high-resolution liquid-state spectrum. In Table 1, we summarized our attempts at such a Lorentzian lineshape fitting to deduce the relative populations. At relatively low speeds, between 20 and 30 kHz, where the MAS averaging was insufficient, a variation of 6% was found for the F2 component. Although, ideally one could spin faster to entirely average the dipolar interactions more effectively, this turned out to be unnecessary. At higher speed above 30 kHz, the line broadening was indeed effectively suppressed, and the determinations at the various MAS speeds resulted in only a 3% variation, which is within our fitting error limits (±3%). In other words, at these high speeds, the averaging effect has reached the ultimate limit that the fitting analysis is unable to distinguish. According to the assignments of liquid-state NMR spectrum reported by Tonelli et al. [6], the relative portion of head-to-head and tail-to-tail defect segments is available from the average population of D1 and D2 components. The above determinations yielded the following relative contents for our PVDF sample: 5% for defect segments; 41% crystalline phases (F1 + F3); and the rest 54% amorphous domains; with ±3% error limits. For the annealed sample the spectrum, shown in Fig. 1d, exhibited considerably broader lines arising from the heterogeneous broadening effect. Notable changes in the populations of the crystalline domains are found (see Table 1).

Table 1
Relative populations for morphological components of PVDF as determined by the lineshape fitting analysis on fast MAS spectrum obtained at various speeds (determined by Lorentzian fitting curve if not specified; line width in Hz is given in bracket; line fitting uncertainty is 3%)

Spinning speed (kHz)	F1	F2	F3	D1	D2
	10.9	55.8	24.6	4.1	4.6
20	(2115)	(1175)	(2272)	(826)	(940)
	12.7	49.2	29.0	3.6	5.6
30	(1880)	(861)	(2115)	(655)	(874)
	9.4	48.9	31.7	3.6	6.5
35	(1723)	(705)	(1993)	(635)	(874)
	1.1[a]	54.2	33.5[a]	4.2	7.0
35[b]	(2024)	(1306)	(3069)	(1059)	(1175)

[a] Determined by Gaussian fitting curve.

[b] Obtained on an annealed sample with process described in experimental section.

3.2. T_1, T_2 and chemical shift anisotropy measurements

Results from spin–lattice relaxation time T_1 measurements and spin–spin relaxation time T_2 measurements are tabulated in Table 2. T_1 values for peaks F1, F2 and F3 components determined by the inversion recovery experiments, are 980, 590 and 840 ms, respectively. In the T_2 measurements, F1 and F3 yielded slightly shorter values of 330 and 400 μs, respectively, compared with 430 μs for F2. As expected, crystalline peaks have slightly longer T_1 and shorter T_2 relaxation times compared with peaks associated with amorphous and defected regions. These observations are consistent with the peak assignments. In order to define their molecular identities further, chemical shift tensor principal values have been deduced from their spinning sideband intensities following the method of Herzfeld and Berger [16]. The fast MAS of 35 kHz 1D spectrum acquired at an extra-high field of ^{19}F Larmor frequency of 752.8 MHz for greater accuracy was shown in Fig. 3. The chemical shift tensor elements retrieved from the spinning sideband intensities are given in Table 3. As expected the amorphous phase has a much smaller shielding anisotropy, possibly effected by an intrinsically more rapid molecular motion, than the shielding anisotropy deduced for the crystalline phases. It is interesting that, in addition to 14.3 ppm chemical shift difference, the two crystalline phases F1 and F3, have different chemical shift tensor elements. It is possible that these large chemical shift tensors are more sensitive to their local chain conformations [10]. Further studies of these shielding tensors and their

Table 2
^{19}F T_1 and T_2 measurements on PVDF rotating sample at 35 kHz

	F1	F2	F3	D1	D2
T_1(ms)	980	590	840	640	630
T_2(μs)	330	430	390	440	480

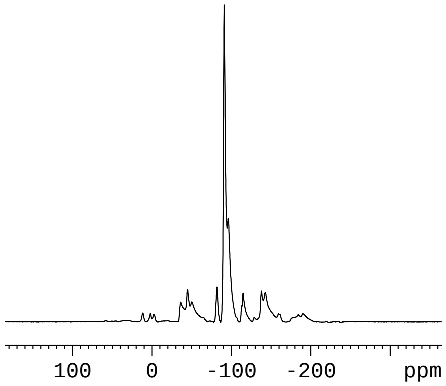

Fig. 3. Solid-state fast MAS ^{19}F spectra acquired at Larmor frequency of 752.8 MHz under 35 kHz.

correlation to molecular structure and molecular packing are under progress.

Table 3
PVDF ^{19}F chemical shift tensor elements in ppm (error limits are ±2 ppm)

	σ_{iso}	σ_{11}	σ_{22}	σ_{33}	$\Delta\sigma$[a]
F1	−81.8	−180	−94	29	166
F2	−91.2	−134	−102	−37	81
F3	−96.1	−171	−101	−16	121

[a] Shielding anisotropy $\Delta\sigma = \sigma_{33} - (\sigma_{11} + \sigma_{22})/2$.

3.3. Molecular proximity studies by 2D exchange spectroscopy

The 2D exchange ^{19}F NMR spectra of PVDF are given in Fig. 4. The cross peaks associated with the two crystalline resonances, and between the amorphous and the defect segments are clearly displayed. It is possible that the cross peaks or exchange signals indicate a molecular chain reorientation process before and after the mixing time [17,18]. Alternatively, they could result from spin diffusion processes occurring in related sites. To distinguish between these two possibilities, we have performed a 2D exchange experiment, with a rotor-synchronized 180° pulse trains added in the mixing period [12]. The 180° pulse trains serve to selectively enhance spin transfer mediated by dipolar interactions. Supposedly, if the cross-peaks or exchange signals were solely due to molecular reorientations, they should have the same intensities regardless of the 180° pulse trains. On the other hand, if the cross peaks arose from spin diffusion, their intensities would be enhanced accordingly. In fact, as shown in Fig. 4b, the cross-peaks increase notably, suggesting a strongly correlated process occurring among associated spins. Apparently, these processes occur between the two crystalline regions, and between the amorphous and the defect segments. Thus, even at fast MAS speed of 35 kHz, the homonuclear dipolar interaction does not completely average out, facilitating the spin diffusion process observed. The effectiveness of the spin dynamic process reflects the molecular proximity in closely related residuals. Based on the lamellae spin-diffusion behavior proposed by Clauss et al. [17] that the two crystalline regions are separated on a scale of nanometres. In ^{2}H NMR studies, crystalline chain conformation exchange has been reported by Hirschinger et al. near the melting point of the polymer [19]. However, no evidence was obtained that showed any correlation between the spin diffusion behavior observed in this work and the chain conformation exchange proposed earlier.

To characterize the molecular packing effects, we have also investigated the origins of line widths in the 2D spectrum. The line broadening along the diagonal in the 2D spectrum arises from both homogeneous (dipolar interactions) and inhomogeneous (molecular packing) effects. Along the direction that is perpendicular to diagonal, the line width is due to homogeneous broadening solely. In Fig. 4a, the crystalline signals give circular shape line

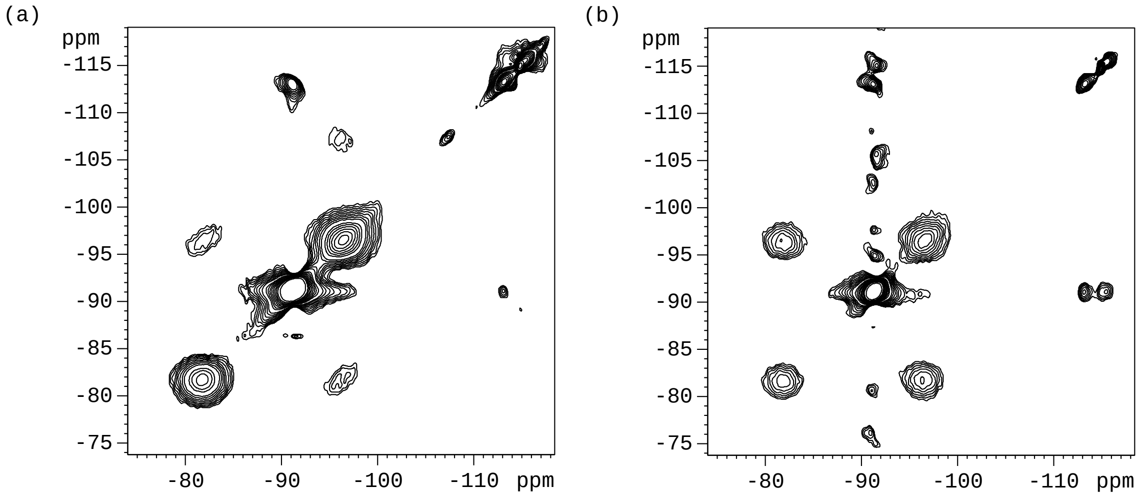

Fig. 4. ^{19}F 2D exchange fast MAS spectra acquired: (a) at 35 kHz with mixing time of 3.5 ms; (b) is same as (a) in presence of the additional 180° pulse trains during mixing period to enhance spin diffusion. The alias signals at −91.2 ppm along the F1 dimension was due to the effect of pulse trains.

broadening pattern indicating that the homogeneous broadening contributes the most. In contrast, the amorphous and the defect signals showed more feature due to inhomogeneous broadening than to homogeneous broadening, implying that a distribution of molecular packing is dominating the observed line broadening effects here.

4. Summary

It has been shown that the fast MAS ^{19}F NMR spectroscopy can be used to quantitatively analyze the relative populations of morphological components in PVDF. Large dispersion in chemical shifts facilitates peak assignments of the three molecular entities in the morphology, namely, crystalline, amorphous domains and defect segments. Two crystalline F1 and F3 components, with a 14.3 ppm difference in chemical shifts, have also been shown to have different chemical shift tensor values. Two-dimensional spin diffusion experiments indicate molecular proximity in morphological components, specifically between the crystalline phases, and between the defect structure and the amorphous regions.

Acknowledgements

The authors would like to thank the Bruker Instruments Co. in Karlsruhe, Germany, for permission to access one of its solid-state Avance spectrometers and fast MAS probes for the experiments described here. We also like to thank Dr J.D. Wright for carefully reading the manuscript. Financial support of the work by the National Science Council, ROC under research grant NSC 88-2623-D-006-013 is gratefully acknowledged.

References

[1] Tashiro K. In: Nalwa HS, editor. Ferroelectric polymers: chemistry, physics, and applications, New York: Marcel Dekker, 1995. chap. 2.
[2] Hasegawa R, Takahashi Y, Chatani Y, Tadokoro H. Polym J 1972;3:600.
[3] Doll W, Lando JB. J Macromol Sci, Phys 1970;B4:309.
[4] Bachmann MA, Lando JB. Macromolecules 1981;14:40.
[5] Schmidt-Rohr K, Spiess HW. Multidimensional solid-state NMR and polymers. Academic Press, 1994.
[6] Tonelli AE, Schilling FC, Cais RE. Macromolecules 1982;15:849.
[7] Ferguson RC, Brame JrEG. J Phys Chem 1979;83:1397.
[8] Maciel GE, Bronnimann CE, Hawkins BW. In: Warren WS, editor. The Waugh Symposium, Adv Magn Reson 1990;14:125.
[9] Gerstein BC, Pembleton RG, Wilson RC, Ryan LM. J Chem Phys 1977;66:361.
[10] Holstein P, Scheler U, Harris RK. Polymer 1998;39:4937.
[11] Takahashi Y, Matsubara Y, Tadokoro H. Macromolecules 1983;16:1588.
[12] Shaka AJ, Keeler J, Freeman R. J Magn Reson 1983;53:313.
[13] Jeener J, Meier BH, Bachmann T, Ernst RR. J Chem Phys 1979;71:4546.
[14] Gullion T, Vega S. Chem Phys Lett 1992;194:423.
[15] Bennett AE, Ok JH, Griffin RG, Vega S. J Chem Phys 1992;96:8624.
[16] Herzfeld J, Berger AE. J Chem Phys 1980;73:6021.
[17] Clauss J, Schmidt-Rohr K, Spiess HW. Acta Polym 1993;44:1.
[18] Schmidt-Rohr K, Spiess HW. Macromolecules 1991;24:5288.
[19] Hirschinger J, Schaefer D, Spiess HW, Lovinger AJ. Macromolecules 1991;24:2428.